HHS Public Access

Author manuscript

Nat Genet. Author manuscript; available in PMC 2016 June 22.

Published in final edited form as:

Nat Genet. 2015 September ; 47(9): 996–1002. doi:10.1038/ng.3361.

Exome sequencing identifies recurrent mutations in *NF1* and RASopathy genes in sun-exposed melanomas

Michael Krauthammer[1,2], **Yong Kong**[3], **Antonella Bacchiocchi**[4], **Perry Evans**[1], **Natapol Pornputtapong**[2], **Cen Wu**[5], **Jamie P McCusker**[2], **Shuangge Ma**[5], **Elaine Cheng**[4], **Robert Straub**[4], **Merdan Serin**[4], **Marcus Bosenberg**[2,4], **Stephan Ariyan**[6], **Deepak Narayan**[6], **Mario Sznol**[7], **Harriet M Kluger**[7], **Shrikant Mane**[8,9], **Joseph Schlessinger**[10], **Richard P Lifton**[9,11], **Ruth Halaban**[4]

[1]Program in Computational Biology and Bioinformatics, Yale University School of Medicine, New Haven, Connecticut, USA

[2]Department of Pathology, Yale University School of Medicine, New Haven, Connecticut, USA

[3]Molecular Biophysics and Biochemistry, Yale University School of Medicine, New Haven, Connecticut, USA

[4]Department of Dermatology, Yale University School of Medicine, New Haven, Connecticut, USA

[5]School of Public Health, Yale University School of Medicine, New Haven, Connecticut, USA

[6]Department of Surgery, Yale University School of Medicine, New Haven, Connecticut, USA

[7]Comprehensive Cancer Center Section of Medical Oncology, Yale University School of Medicine, New Haven, Connecticut, USA

[8]Yale Center for Genome Analysis, Yale University School of Medicine, New Haven, Connecticut, USA

[9]Department of Genetics, Yale University School of Medicine, New Haven, Connecticut, USA

[10]Department of Pharmacology, Yale University School of Medicine, New Haven, Connecticut, USA

[11]Howard Hughes Medical Institute, Yale University School of Medicine, New Haven, Connecticut, USA

Correspondence should be addressed to R.H. (ruth.halaban@yale.edu) or M.K. (michael.krauthammer@yale.edu).

Accession codes. The entire data set has been deposited in dbGAP under accession number phs000933.

Note: Any Supplementary Information and Source Data files are available in the online version of the paper.

AUTHOR CONTRIBUTIONS

M.K. and R.H. designed and performed the research, analyzed and interpreted the data, and wrote the manuscript. R.P.L. and J.S. designed the experiments. A.B., E.C., R.S. and M. Serin conducted the experiments. M.K., Y.K., P.E., J.P.M., S. Mane and N.P. analyzed the data from whole-exome sequencing. S. Ma and C.W. performed statistical analysis. M.B. evaluated the tumor percentage in the clinical specimens. S.A., D.N., M. Sznol and H.M.K. provided the clinical specimens and clinical annotation, as well as input in writing the manuscript.

COMPETING FINANCIAL INTERESTS

The authors declare no competing financial interests.

Abstract

We report on whole-exome sequencing (WES) of 213 melanomas. Our analysis established *NF1*, encoding a negative regulator of RAS, as the third most frequently mutated gene in melanoma, after *BRAF* and *NRAS*. Inactivating *NF1* mutations were present in 46% of melanomas expressing wild-type *BRAF* and *RAS*, occurred in older patients and showed a distinct pattern of co-mutation with other RASopathy genes, particularly *RASA2*. Functional studies showed that NF1 suppression led to increased RAS activation in most, but not all, melanoma cases. In addition, loss of *NF1* did not predict sensitivity to MEK or ERK inhibitors. The rebound pathway, as seen by the induction of phosphorylated MEK, occurred in cells both sensitive and resistant to the studied drugs. We conclude that NF1 is a key tumor suppressor lost in melanomas, and that concurrent RASopathy gene mutations may enhance its role in melanomagenesis.

Recent years have seen unprecedented growth in the understanding of genetic and genomic changes in melanoma. Much of the information is from next-generation sequencing (NGS), particularly exome sequencing, and has been instrumental in the discovery of new cancer-driver genes. These NGS studies have corroborated the previously identified frequent recurrent somatic mutations in *BRAF* and *NRAS* and revealed new melanoma mutations, including a recurrent mutation in *RAC1* (*RAC1*^{P29S}), the third most frequent activating mutation in sun-exposed melanoma after *BRAF* and *NRAS*, and the most frequent recurring mutation in the Rho GTPase family[1–3]. The mutant protein RAC1^{P29S} is a fast-cycling GTPase favoring the GTP-bound state that accelerates cell proliferation and migration when expressed in normal melanocytes. Screens uncovered other mutations at recurrent positions in *PPP6C* that reduce the phosphatase's catalytic activity, consequently dysregulating the kinase AURKA and causing chromosome instability[4,5]. Frequent inactivating mutations were also discovered in the tumor suppressors *TP53, NF1* and *ARID2*, and less frequent mutations were found in *TACC1, GRM3, MAP3K4* and *MAP3K9* that are likely to enhance melanoma pathogenesis[6,7]. Furthermore, recent studies have shed light on variants in regulatory regions of the melanoma genome. Recurrent mutations in the *TERT* promoter, which alter a transcription factor–binding motif and possibly lead to increased expression of TERT, shield melanoma cells from senescence[8,9]. NGS has also fostered an increased understanding of the genetics of noncutaneous melanomas, with the discovery of frequent mutations in *BAP1, EIF1A*X and *SF3B1* in uveal melanoma[10,11].

We report here the results of WES analysis of 213 human melanoma samples, including samples from 109 patients that we studied previously[3] (Supplementary Data). Matched normal DNA was sequenced and analyzed from 133 of the tumors. We also tested the response of melanoma cell lines to the MEK inhibitor selumetinib (AZD6244), currently in clinical trials, and to the ERK inhibitor SCH772984 and performed protein blot analyses to correlate the effects of specific mutations with drug response.

RESULTS

Identification of *NF1*-mutant melanoma subgroup

Nevi can harbor activating *BRAF* or *NRAS* mutations but remain in a growth-arrested state. In some melanomas, somatic mutations in *PTEN, CDKN2A* or *PPP6C* are likely to

account for initiation of the proliferative state. To comprehensively understand the mutations that lead to malignant transformation, we analyzed genes for evidence of selection and significantly increased mutation burden. We applied the '20/20 rule' to identify genes with nonsilent mutations at recurrent positions that constituted 20% or more of all observed mutations or genes with at least 20% inactivating mutations, that is, nonsense, splice-site variant or insertion-deletion (indel) mutations[12]. The top 40 ranked genes from this analysis are shown in Table 1 (details are also provided in the Supplementary Data). Among those, we identified 11 genes that exhibited statistically significant mutation counts above what was expected on the basis of a driver gene analysis by MutSigCV[13] (Fig. 1 and Supplementary Data).

Three genes were mutated with an incidence greater than 10%: *BRAF* and *NRAS*, with known recurrent activating mutations, and *NF1*, with a high number of inactivating mutations. In our cohort, we observed $BRAF^{V600}$ mutations in 38.5% of melanomas (82 of 213) and $RAS^{Q61/G12/G13}$ mutations (58 *NRAS* and 3 *HRAS*) in 28.6% (61 of 213), and two melanomas were *BRAF-NRAS* double mutants (Table 2). Ninety percent of the *NF1*-mutant melanomas (38 of 42) harbored mutations of the inactivating or predicted damaging type (Supplementary Fig. 1 and Supplementary Data), with the majority (26 of 38) in melanomas expressing wild-type *BRAF-RAS*, as noted previously by our group[3] and recently by The Cancer Genome Atlas (TCGA) consortium[14]; two $NRAS^{Q61R}$-mutant, one $KRAS^{G12I}$-mutant and nine $BRAF^{V600}$-mutant melanomas had concurrent *NF1* mutations. Among the tumors with no detectable *BRAF* or *RAS* mutation, a total of 46.4% (26 of 56) were *NF1* mutants (Table 2). Of those, more than 80% (21 of 26) either showed loss of heterozygosity (LOH) across the *NF1* locus or were compound heterozygotes harboring two *NF1* mutations. Conversely, of the 12 *BRAF*-mutant or *RAS-NF1* double-mutant melanomas, one-third (4 of 12) showed LOH or compound heterozygosity (Supplementary Data).

NF1-mutant melanomas harbored significantly more somatic mutations ($P = 1.5 \times 10^{-10}$) and occurred in significantly older patients ($P = 0.017$), but they were associated with similar overall patient survival compared to *BRAF*-mutant, *RAS*-mutant and 'triple–wild-type' (*BRAF-RAS-NF1*–wild-type) melanomas (Fig. 1 and Supplementary Fig. 2).

Mutations in known melanoma-driver genes affecting cell proliferation and survival, including *RAC1, PTEN, CDKN2A, MAP2K1* and *RB1*, were also detected. This list included the X-chromosome gene *FAM58A*, which harbored several inactivating mutations. FAM58A (also known as cyclin M) negatively regulates RAF1 expression via interaction with CDK10, and mutations in *FAM58A* cause the inherited human developmental disease STAR syndrome[15]. Early-termination alterations in FAM58A were present in four tumors from male patients. All of the tumors were *BRAF-RAS* wild type; two were *NF1*-mutant and the other two were triple–wild type. The analysis also showed a recurrent R18W mutation in *BCL2L12*, which encodes an anti-apoptotic factor[16]. This mutation was adjacent to F17F, a recurrent silent mutation with increased inhibitory potential against UV-induced apoptosis due to increased *BCL2L12* gene transcript and protein levels[17].

Mutations in genes involved in chromatin modification or DNA repair were identified, some for the first time in melanoma. The list included two SWI/SNF family members, *ARID1A* (linked to gastric cancers[18]) and *ARID2*, reiterating the role of chromatin remodeling in malignancy. An additional gene in this category was the polycomb protein–encoding gene *EZH2*, which is upregulated in melanoma[19]; we noted recurrent *EZH2*^{Y646N} mutations in four tumors. The mutation was located in the SET domain, which is involved in histone methylation[20]. A considerable number of inactivating mutations were in histone modifiers. Mutations were identified in *KMT2B (MLL2)* and *SETD2*, the latter of which is a recognized tumor suppressor in renal cell carcinoma[21], as well as in *TRRAP*, involved in histone acetylation, which showed a previously described recurrent *TRRAP*^{S722F} mutation[22].

Finally, in the metabolism category, we found 22 mutations in *CYP7B1*, some of which occurred at recurrent positions (H286Y, E321K and P338S), suggesting an important role for cytochrome P450 in melanoma. Diminished expression of CYP7B1 is associated with breast cancer, possibly through modification of cholesterol metabolism[23]. We also observed a recurrent *IDH1*^{R132C} mutation in four tumors. *IDH1*^{R132C}, frequently present in glioma[24] is a neomorphic mutation that causes production of D-2-hydroxyglutarate rather than the normal product, α-keto glutarate[25].

NF1-mutant melanomas harbor co-mutations in RASopathy genes

A search for subtype-specific variants showed that damaging mutations in *RASA2*, which encodes a GTPase-activating protein that suppresses RAS function[26], were exclusively present in *NF1*-mutant melanomas that were *BRAF-RAS* wild type ($P = 0.006$; Supplementary Data). Of the nine *RASA2* mutations, two were nonsense and three were recurrent at position R551C. Four of the seven *RASA2*-mutant tumors showed LOH across the locus (all with a single *RASA2* mutation), and two were compound heterozygotes. The recurrent *RASA2*^{R511C} variant was recently described in the germline of a patient with Noonan syndrome[27], a RASopathy otherwise linked to mutations in *SOS1, PTPN11, RAF1* and other genes affecting RAS-MAPK signaling[28]. A search across these genes showed that four *NF1*-mutant, *BRAF-RAS*–wild-type melanomas harbored disease-causing mutations in *PTPN11*, with p.Tyr279Cys, p.Ala461Thr, p.Pro491Leu and p.Glu506Pro linked to the Noonan and LEOPARD syndromes[29,30]. Two *NF1*-mutant, *BRAF-RAS*–wild-type melanomas harbored mutations in *SOS1* linked to Noonan syndrome (p.Gly434Arg and p.Arg552Lys)[31–33], and another two had mutations in *RAF1* (p.Pro261Leu and p.Thr491Ile) that were also associated with Noonan syndrome[34]. *NF1*-mutant melanomas also featured mutations in *SPRY* and Sprouty-related genes known to encode negative regulators of MAPK signaling. In particular, three *NF1*-mutant melanomas harbored protein-coding alterations in *SPRED1*, including early-termination mutations. SPRED1 enhances NF1 activity by recruiting the protein to the plasma membrane[35], and early-termination mutations in *SPRED1* are linked to Legius syndrome (another RASopathy), which is characterized by neurofibromatosis- like skin features such as multiple café-au-lait macules, but not neurofibromas[36].

In all, out of 26 *NF1*-mutant, *BRAF-RAS*–wild-type melanomas, ~60% (15) carried mutations in known RASopathy genes *RASA2, PTPN11, SOS1, RAF1* and *SPRED1*, the majority of which (10 of 15) were documented disease-causing mutations (Table 3 and Supplementary Data).

Although the occurrence of RASopathy gene mutations was significantly associated with *NF1*-mutant, *BRAF-RAS*–wild-type melanomas ($P = 0.0004$; Supplementary Data), 8.6% (16 of 187) of the remaining melanomas in our cohort also featured mutations in these genes (Supplementary Fig. 3). Mutations in three of these genes were thought to be disease causing: (1) two early-termination mutations in *SPRED1* (in two different tumors, one with $BRAF^{V600E}$ and another with $NRAS^{Q61L}$ mutation); (2) p.Asn58Ser in *PTPN11*, a known gain-of-function mutation in lung cancer[37] that occurred in a melanoma with $NRAS^{Q61R}$; and (3) a p.Met269Lys *SOS1* mutation in a triple–wild-type melanoma. The mutated residue in *SOS1* (p.Met269) has documented associations with Noonan syndrome[38].

Of interest, the pathogenic $PTPN11^{P491L}$ and $MAPK1^{D321V}$, the latter a mutation in the docking site for DUSP-ERK interaction, were present in YUKLAB $NF1^{H729Q/R1204W/R416*}$ melanoma. The protein encoded by $MAPK1^{D321V}$ is similar to the known D321N, which impairs binding to DUSPs and reduces the sensitivity to inactivation by phosphatases[39]. Finally, two *NF1*-mutant melanomas (YUROG $NF1^{Q1218*}$ and YUCAS $NF1^{FS\text{-}Indel}$) contained $KRAS^{A146T}$ and $KRAS^{Q22K}$, respectively, known activating mutations in colorectal cancer[40].

NF1 mutations, NF1 expression and RAS activation

NF1 negatively regulates RAS by enhancing its RAS GTPase activity, converting active RAS-GTP to inactive RAS-GDP. We therefore investigated NF1 expression and NRAS activity in our exome-sequenced melanoma cell lines. Protein blot analysis showed that 75% of *NF1*-mutant melanomas (six out of ten), all *BRAF-NRAS* wild type, did not express NF1 or expressed it at low levels (Fig. 2a and Supplementary Fig. 4). One melanoma, YUDAB, homozygous for $NF1^{F1464L}$ mutation, did not express the protein, perhaps because of protein instability. Interestingly, the two *NF1*-mutant melanomas that expressed NF1 were also $BRAF^{V600E}$ mutants. One of them was from a neurofibromatosis patient with a germline *NF1* frameshift mutation. This sample showed levels of NF1 expression about half those found in normal human melanocytes (YUSAMIR; Fig. 2a). Figure 2 also shows that two *NF1*–wild-type melanomas (YUHOIN and YUDATE) did not express NF1, and both showed LOH across the NF1 locus.

RAF pulldown assay showed that loss or low levels of NF1 were associated with the presence of activated GTP-bound RAS in most but not all cases (Fig. 2b,c), demonstrating the likely involvement of other RAS regulators.

NF1 expression and drug response

One of the main goals of identifying driver mutations in cancer is to make it easier to choose an appropriate targeted therapy, such as vemurafenib or dabrafenib, drugs that inhibit mutant BRAF melanomas, for the treatment of patients with $BRAF^{V600}$-mutant tumors[41,42]. Loss of NF1 expression was suggested to mediate resistance to the MEK inhibitor selumetinib

(AZD6244) in one report[43] and to be a biomarker for high sensitivity to the MEK inhibitor PD0325901 in another[44]. A more recent study showed that NF1-negative and NF1-positive melanoma cell lines display the same sensitivity to the MEK inhibitor trametinib[45]. We therefore tested the effect of selumetinib, which is currently in clinical trials, on a panel of 21 melanoma cell lines, 10 *NF1* mutants (or null by LOH) and 11 *NF1* wild type, all characterized by exome sequencing (Fig. 3). The data showed that 60% of the *NF1*-mutant melanoma cell lines (six out of ten) were highly sensitive (IC_{50} of 0.036 μM or below), and four were highly resistant (IC_{50} of 2.1–10 μM) (Fig. 3a), indicating that suppression of *NF1* is not always associated with sensitivity or resistance to a MEK inhibitor as was previously suggested[43,44]. Seven of the ten *NF1*-mutant, *BRAF-NRAS*–wild-type melanoma cell lines did not express NF1 or expressed it at extremely low levels (Fig. 2a). Of those, ~43% (three out of seven) were sensitive to MEK inhibition.

All three double-mutant melanoma cell lines in this panel were sensitive to selumetinib. These included YURKEN, which carries $NF1^{P228S}$-$BRAF^{V600E}$ mutation (IC_{50} = 0.028); YUTICA, which harbors $NF1^{P166L}$-$NRAS^{Q61R}$ mutation; and YUSAMIR, an $NF1^{FS}$ indel–$BRAF^{V600E}$ mutant from a person with neurofibromatosis (Fig. 3a). All three expressed high levels of NF1 (Fig. 2a). Also, YURKEN was highly resistant to the BRAF inhibitor vemurafenib, whereas YUSAMIR was highly sensitive to the drug (Supplementary Fig. 5). The results suggest that patients with double mutations should not be *a priori* excluded from vemurafenib treatment on the basis of expected resistance to the drug[43,44].

Melanoma cell lines that did not carry an *NF1* mutation showed diverse sensitivity to selumetinib, with an IC_{50} range of 0.003–0.374 μM, and ~55% (6 of 11) showed only a cytostatic response (Fig. 3b).

We also tested the response to SCH772984, a selective ATP-competitive ERK inhibitor that is in phase I clinical trials. Again, the highly selumetinib-resistant NF1-null YUHOIN and YUHEF melanoma cells were also the most resistant to this ERK inhibitor (Fig. 3c). However, in general, drug response followed a similar distribution in the NF1-null, triple–wild-type and *BRAF-NRAS* mutant melanoma cell lines (Fig. 3c,d).

We explored the possibility that selumetinib induces upstream-pathway activation that is more prominent in NF1-null resistant cells than in sensitive cell lines, as this was suggested to characterize MEK resistance[44]. Protein blot analyses showed increased levels of phosphorylated MEK (pMEK) in all melanoma cells that did not carry the $BRAF^{V600E/K}$ mutation (i.e., NF1-null, $NRAS^{Q61R/L}$-mutant and even normal human melanocytes), regardless of the cells' sensitivity to selumetinib in cell proliferation assays (Fig. 4a,b). Furthermore, although pERK was suppressed within an hour in response to selumetinib in all cell lines, its rebound at later time points was not indicative of resistance to the drug. For example, pERK did not recover in the resistant YUHEF cell line at the end of 24 h of treatment with 100 nM selumetinib, whereas it did recover in the resistant YUSOC and YUHOIN lines, as well as in the sensitive cell line YUDAB (Fig. 4a). Taken together, the data show that the feedback that leads to ERK activation in response to selumetinib in NF1-null melanoma cells is not necessarily associated with resistance to the drug, and that pERK phosphorylation is not required for selumetinib resistance.

Somatic copy-number alterations in triple–wild-type melanomas

We derived the genomic copy-number status and somatic copynumber alterations (SCNAs) on the basis of differences in read coverage between normal and matched tumor samples. Recent bioinformatics approaches allow for the long-range prediction of SCNAs by means of exome sequencing[46]. The corresponding SCNA segments can then be analyzed for broad and focal amplified and deleted regions with downstream programs such as GISTIC[47]. The GISTIC results for our matched melanoma samples are listed in the Supplementary Data and are presented graphically in Supplementary Figure 6. We observed known deletions in 9p21.3 (*CDKN2A*), 17p13.1 (*TP53*) and 10q23.31 (*PTEN*) and amplifications in 1q31.3 (*ASPM*) and 7q34 (*BRAF*). We identified a significant amplification signal in 7p22.1, near the *PMS2* locus, and an amplification peak in 5p15.33, which harbors *TERT*. The latter supports the role of telomerase maintenance in melanoma based on recurrent somatic mutations in the *TERT* promoter[8,9].

We also conducted GISTIC analysis with a focus on triple–wild-type melanomas, specifically, 19 matched melanomas that were wild type for *BRAF, RAS* and *NF1*. The analysis revealed a distinctive amplification peak at 4q12, harboring the *KIT-KDR* locus (Supplementary Fig. 7) that was present in two melanomas. KIT and KDR are receptor tyrosine kinases that activate the MAPK pathway[48,49]. Triple–wild-type melanomas carried additional characteristic copy-number alterations, including an amplification peak in *MAP3K8* in YUROL that was not seen in any other melanoma specimen (Supplementary Fig. 8a,b). MAP3K8 expression has been implicated as a resistance mechanism to BRAF-inhibitor therapy in melanoma[50]. Another amplification peak was seen in YUDATE melanoma that included the *MAPK1* (*ERK2*) locus (Supplementary Fig. 8c).

DISCUSSION

The genome-wide mutational analysis of melanoma reinforces the role of known frequent mutations in this devastating cancer and enhances our understanding of the processes that lead to melanomagenesis. This study showed that sun-exposed melanomas harbored a large number of missense mutations, but only a few were of the gain-of-function type characteristic of oncogenes such as *BRAF, NRAS, RAC1, MAP2K1, EZH2* and *IDH1* that are amenable to targeted therapy. In fact, mutations at recurrent positions can be of the inactivating type, as was demonstrated for PPP6C[5]. The majority of the loss-of-function changes affect processes involved in cell cycle progression; chromatin remodeling, DNA repair and/or transcription including histone methyltransferases (*KMT2A*, SETD2); and members of the SWI/SNF complex (ARID2 and ARID1A). Together these changes are likely to modify gene expression that releases normal cellular safeguards or constraints for which the design of inhibitors is more challenging.

The results of our large-scale exome sequencing highlight NF1 as a major player in melanomagenesis. In our cohort, 46% of *BRAF-RAS*–wild-type melanomas harbored *NF1* mutations, which are often associated with LOH due to hemizygous deletions or copy-neutral gene conversions, or carried two or more single-nucleotide variants, suggesting biallelic mutation. *NF1-BRAF* and *NF1-RAS* double-mutants displayed considerably less LOH and fewer biallelic *NF1* mutations (4 out of 12) than did *NF1*-mutant, *BRAF-RAS*–

wild-type melanomas (21 of 26), and when tested they were found to express normal or high levels of NF1, suggesting a minor role for this tumor suppressor in these melanomas. In contrast, all of the *NF1*-mutant, *BRAF-NRAS*–wild-type melanomas did not express NF1. The loss of NF1 expression led to increased RAS activation in most but not all of these cases; RAS relative activity remained low in two out of the six NF1-null melanoma cell lines, probably because of the effects of other RAS-GTPase–activating proteins.

We found that NF1-null melanoma cell lines could be either sensitive or resistant to MEK or ERK inhibitors. We searched for additional mutations that may confer resistance to these inhibitors by activating alternative signaling pathways. Two of the three selumetinib-resistant *NF1*-mutant melanomas also carried the *RAC1*^{P29S} mutation (YUHEF and YUSOC), in line with a recent publication indicating that RAC1mutant melanomas are relatively resistant to MEK inhibitors[51]. However, the YUTOGS melanoma is also a *RAC1*^{P29S}-*NF1* double-mutant but was highly sensitive to selumetinib (IC_{50} = 0.022 μM). We speculate that other damaging mutations could facilitate activation of the phosphoinositide 3–kinase (PI3K)-mTOR pathway. For example, YUHEF melanoma carries three mutations in the RASopathy gene *SOS1* (p.Pro102Ser, p.Arg398Gly and p.Gly434Val) that may confer constitutive RAS activity, and *PHLPP2* mutations are present in YUSOC (p.Pro142Ser) and YUHEF (p.Ser915Phe). PHLPP1 and PHLPP2 (similar to PTEN, which was not altered in these cells) are phosphatases that target AKT, PKC, S6K and RAF1, and their inactivation has been demonstrated in other cancers[52]. Furthermore, downregulation of PHLPP1 increases AKT activity, enhances the proliferation of melanoma cells and melanocytes and results in anchorage-independent growth of melanocytes[53].

Neurofibromatosis is a genetic disorder that affects the nervous system and causes benign cutaneous neurofibromas and elevated risk for multiple Schwann cell tumors[54]. Epidemiological studies show that there is a general increase in the incidence of 13 other cancers among people with neurofibromatosis, albeit at a much lower rate, and melanoma is one of them[55]. Interestingly, melanocytes from café-au-lait macules of NF1 patients carry a somatic or second-hit mutation in *NF1*, indicating that a loss of NF1 provides a growth stimulus to normal melanocytes but does not accelerate their malignant transformation[56]. One possibility is that NF1 loss may be a more effective NRAS activator in the nervous system than in melanocytes[57]. Another likely explanation may relate to the timing of the mutation, with inherited loss of *NF1* leading to the neurofibromatosis phenotype, and somatic mutations later in life, accompanied by additional alterations, leading to a variety of human cancers[58]. A similar observation has been made for retinoblastoma: although small-cell lung cancers show some of the highest somatic *RB1* mutation rates, long-term retinoblastoma survivors with *RB1* germline mutations have only a slightly increased incidence of secondary lung cancers[59].

We identified documented disease-causing mutations in RASopathy genes *RASA2, PTPN11, SOS1, RAF1* and *SPRED* predominantly in *NF1*-mutant melanomas, but also in *BRAF-RAS* mutant and triple– wild-type tumors, to a lesser degree. To our knowledge this is the first report to describe the presence of several known RASopathy gene mutations in melanoma, highlighting a possible role for these altered genes in cancer pathogenesis. Most of these mutations are found in *NF1*-mutant melanomas, and our functional studies

showed that a loss of NF1 expression did not always lead to NRAS activation. These results raise the intriguing possibility that *NF1*-mutant melanomas may require additional changes for robust MAPK pathway activation. Indeed, clinically, concurrent *NF1* and *PTPN11* mutations cause severe or lethal forms of Noonan syndrome[60,61]. There is a case of a child with concurrent *NF1* and *PTPN11* mutation who developed bilateral optic nerve glioma, whereas the remaining family members, who carried only an *NF1* mutation, displayed mild neurofibromatosis symptoms (café-au-lait spots)[62]. In addition, there is evidence that a loss of NF1 expression enhances the activity of noncanonical RAS mutations[63], which is relevant to our observation of two cases of *NF1*-mutant melanomas, one with $KRAS^{A146T}$ mutation and the other with $KRAS^{Q22K}$ mutation.

ONLINE METHODS

Melanoma tumors and cell cultures

Normal human melanocytes (NBMEL) were cultured from foreskins of newborn males. The foreskins were incubated in dispase overnight at 4 °C, and epidermal melanocytes were further dissociated after 10 min of incubation in 0.25% trypsin-EDTA solution (GIBCO-Life Technologies). The cells were sedimented, and the pellets were incubated in OptiMEM (GIBCO), 5% FCS (Gemini Bio-Products), 1% Pen Strep (GIBCO) supplemented with 10 ng/ml basis fibroblast growth factor (ConnStem, F1001), 1 ng/ml heparin (Sigma, H3393), 0.1 mM dbcAMP (Sigma, D-0627) and 0.1 mM 3-isobutyl-1-methylxanthine (Sigma, I-5879). Melanoma tumors were excised to alleviate tumor burden, and cells were cultured in OptiMEM plus 5% FCS and Pen Strep. Specimens were collected by the Tissue Resource Core of the Yale SPORE in Skin Cancer with participants' informed signed consent according to Health Insurance Portability and Accountability Act (HIPAA) regulations with a Human Investigative Committee protocol. The melanomas used for sequencing were from snap-frozen tumors or from short-term cell cultures[64]. The cell cultures were routinely checked for mycoplasma contamination and were discarded when they tested positive. Matching normal DNA was obtained from circulating lymphocytes or normal skin.

DNA extraction

The DNeasy purification kit (Qiagen, Valencia, CA) was used to extract DNA from cell pellets and freshly frozen tumors. The OneStep PCR Inhibitor Removal Kit (Zymo Research Corporation, Irvine, CA) was used to remove melanin from highly pigmented samples.

Exome sequencing data analysis

SNV and indel calling; somatic versus novel variants—We followed a previously described protocol for read alignment, single-nucleotide variant (SNV) and indel calling, data filtering, and somatic calling[3]. In short, we used the bwa program for read mapping and SAMtools for SNV calling[65,66]. SNVs were filtered according to the following quality criteria: (i) mutant allele frequency of ≥13%; (ii) SAMtools mapping score of ≥40; (iii) at least one forward and one backward read; and (iv) a minimum coverage of four mutant and eight total reads at the variant position. An SNV was called somatic in the absence of variant reads in the germline DNA samples, with one mutant read tolerated in the normal samples, and expecting a sufficient variant-to-total-read ratio in tumor and normal samples

as assessed by Fisher's exact test (*P* value threshold of 0.001). Generated data are with respect to Genome Reference Consortium human genome build 37 (GRCh37).

Somatic versus novel mutations—For our samples for which we had both tumor and matched germline DNA, we derived somatic SNVs, splice variants (SVs) and indels. For the entire cohort of matched and unmatched samples, we derived all SNVs, SVs and indels that were determined to be 'novel', i.e., not found in repositories of common human variation (phase 1 data from the 1,000 Genome Project and 2,577 non-cancer exomes sequenced at Yale) at a frequency of less than 0.05% and therefore enriched in somatic and private inherited mutations. We used the somatic mutations for the MutSigCV analysis and to calculate whether a gene had at least 20% somatic mutations at recurrent positions or at least 20% inactivating somatic mutations (integrating somatic data from the Broad Institute of MIT and Harvard and TCGA screens[66]). We used the list of mutations that were novel and predicted to be damaging for identifying paired and unpaired samples with mutations in driver genes, and for detecting gene mutations associated with the NF1 subgroup (redistribution analysis, discussed below). For all calculations that compare mutations counts across samples, we restricted the counts to genes with consistent coverage across samples.

Integrated mutation data from the Broad Institute of MIT and Harvard and TCGA—We integrated melanoma data from a recent publication by the Broad Institute[2], and from the TCGA project[66]. For the TCGA project, we downloaded the automated somatic calls provided by the Baylor College of Medicine (4/17/2014) and Broad Institute (3/22/2014), available at the TCGA data portal. Both projects provided the data in MAF format. We removed samples that were in common between the data sets before integrating the data by calculating the overlap in somatic mutations between the cohorts and removing samples that shared a majority of mutations with another screen. After consolidation, we created an integrated data set of 397 melanomas from the Broad and TCGA cohorts.

Redistribution analysis for identifying co-mutated genes—To identify genes that were significantly co-mutated across the melanoma subgroups, we first applied the χ^2 test to the equality of mutation counts across the four groups (*NF1, BRAF, RAS* and wild type). We additionally performed a redistribution analysis by adjusting for the total number of mutations (n_t) per group. For each gene, we first computed the weighted mutation counts, or expected counts, for each group with weights n_1/n_t, n_2/n_t, n_3/n_t and n_4/n_t, respectively, where n_1, n_2, n_3 and n_4 are the total number of mutations per group and $n_t = n_1 + n_2 + n_3 + n_4$. Then a scalar was multiplied by the weighted counts to ensure that the total number of counts for the gene stayed the same before and after redistribution. A χ^2 test was then performed to determine whether the redistribution counts were equal across the four groups. For final selection, we filtered for genes with a redistribution analysis FDR of <0.2 (Supplementary Data). We performed a similar analysis to calculate whether the set of RASopathy genes were associated with the *NF1* subgroup by tallying the mutation across the RASopathy genes and performing a redistribution analysis (Supplementary Data).

Gene mutation burden analysis: 20/20 rule—We calculated the top mutated and expressed genes on the basis of a heuristic rule[12] that selects genes in which 20% or more

of the observed somatic mutations are at recurrent sites, or in which 20% or more of the observed somatic mutations are inactivating (i.e., nonsense, splice-site, or indel). To increase power, we decided to integrate the somatic calls from the Yale cohort with the somatic calls from the integrated Broad-TCGA cohort for candidate gene identification. Genes with >20% somatic mutations and at least 1% frequency in the combined cohort were then ranked by the incidence of novel mutations in the entire Yale cohort (Table 1 and Supplementary Data).

Gene-mutation burden analysis using MutSigCV—The list of driver genes was identified using MutSigCV (Version 1.4)[13], which distinguishes significantly mutated genes from others by taking into account mutational heterogeneity caused by replication timing, gene expression levels and chromatin state. We ran MutSigCV using the default input files as provided by the MutSigCV download page and prepared the mutational data using a MAF file comprising the somatic calls of expressed genes across the 133 matched samples of the Yale cohort. We selected significantly mutated genes using an FDR threshold of <0.2 among all genes that had at least one somatic mutation.

Survival analysis across the melanoma subgroups—We carried out an analysis to determine whether mutational status (*NF1, BRAF, RAS* and wild type) is associated with melanoma survival. The analysis was done for four mutational groups (*NF1* mutant versus *NF1* wild type, $BRAF^{V600}$ versus *BRAF* wild type, *RAS* mutant versus *RAS* wild type, and *BRAF-RAS* wild type versus *BRAF-RAS* mutant). We considered two types of survival times by taking into account (1) the difference between age at last encounter and age of metastasis onset, and (2) the difference between age at last encounter and age of primary onset. The survival times and vital status were then used to obtain Kaplan-Meier curves. The analysis was done both with and without adjustment for age; for example, for the *NF1* mutant–versus–wild type group analysis (age of metastasis onset), the *P* values with and without adjustment for age effects were 0.216 and 0.241, respectively.

CNV analysis—We used Excavator (Version 2.1)[46] and GISTIC (Version 2.0.16)[47] to calculate significantly amplified or deleted regions. Excavator was run with the default settings. The resulting chromosome-level segmentation data (genomic intervals), together with the location of the exome probes, were then used in GISTIC to generate the copy-number results. GISTIC was run with parameters of logR threshold for calling a segment amplified of ±0.25 and capping logR values at 2.

Tumor-purity calculation

We calculated sample purity in our paired samples by two approaches. The first approach was based on mutant allele frequency (MAF) estimation in regions of LOH. First, we established all LOH regions using the R module DNACopy. For each LOH region, we determined the median MAF for heterozygous inherited SNVs. We then used $2|0.5 - MAF|$ as a proxy for purity. Second, for samples with no LOH, we assumed that the majority of somatic mutations were heterozygous and used two times the median MAF of somatic mutations as a proxy for purity.

Automated tumor-purity calculation of our 133 paired samples showed a mean tumor-purity value of 0.63 ± 0.21, with 1.0 being the value of pure samples (Supplementary Data). Purities as low as 26% would theoretically be sufficient for calling heterozygous mutations with our mutation-calling thresholds and level of coverage. Review of selected samples and/or slides by a pathologist showed agreement with the automated analysis, with a mean purity of 71.7% across 24 paired and unpaired samples (Supplementary Data).

Sequencing statistics

For our tumor samples, we calculated a mean error rate of 0.2% ± 0.08% per called SNV, a mean coverage of 204 ± 76 independent reads per base, and coverage of at least eight independent reads across 96.5% ± 3% of the covered bases. Our matched normal samples were sequenced with a slightly smaller coverage of 141 ± 42 independent reads per base.

Variant-call precision

We Sanger validated 418 novel SNVs that were called using our variant-calling pipeline. We measured a precision of 93%, corresponding to 389 true positive and 29 false positive variant calls.

Protein blot analyses

Cell pellets were lysed in RIPA buffer supplemented with protease and phosphatase inhibitors, and the levels of proteins were estimated with the Bio-Rad kit (Bio-Rad Laboratories). For NF1 analysis, cell extracts from different melanomas (20 μg/lane) were subjected to protein blot analysis with a 3%–8% Tris-acetate gel, Tris-acetate SDS running buffer and NuPAGE transfer buffer (Life Technologies, NP0006). The membranes were probed with anti-NF1 (Bethyl Laboratories, A300-140A) followed by anti–β-actin monoclonal antibody (clone AC-74, A5316, Sigma-Aldrich) as a control for protein loading. For MEK signaling pathway analysis, normal human melanocytes and melanoma cells were either untreated or treated with 100 nM selumetinib (Selleckchem Chemicals, S1008). Cells were harvested 1, 6, and 24 h later, and cell lysates were subjected to protein blot analysis in 4–12% Bis-Tris gels (Novex) as described[64]. The antibodies used were to phospho-MEK1/2 pSer217/221 (9121), MEK1/2 (4694), phospho-ERK2 pThr202/Tyr204 (9106), and ERK1/2 (4695), all from Cell Signaling Technology.

Analysis of intracellular RAS-GTP

We analyzed the RAS activation state with the Active RAS Pull-Down and Detection Kit from Thermo Scientific (16117) according to the manufacturer's instructions. Cell lysates (400 μg protein) were incubated with GST-bound RAF1-RAS binding domain (GST-RAF1-RBD), and the levels of RAS-GTP were evaluated by protein blotting of bound material with anti-NRAS (or anti-panRAS). Whole-cell lysates (20 μg) were loaded in parallel to estimate the input levels of NRAS. The levels of active NRAS were estimated by band intensity relative to total NRAS, measured using the NIH software ImageJ 1.46r and normalized to *NRAS*^{Q61R} YUFIC melanoma.

Cell proliferation assays

Cell proliferation assays were performed in 96-well plates with the CellTiter-Glo Luminescent Cell Viability Assay in triplicate or quadruplet wells, measured at the end of 72 h of treatment with increasing concentrations of selumetinib, SCH772984 (Selleckchem Chemicals, S7101), or the $BRAF^{V600}$ inhibitor vemurafenib (PLX4032, Plexxikon). The IC_{50} values (drug concentrations that reduced cell viability to 50% of the control) were calculated from the slope of the drug response generated in GraphPad Prism.

Supplementary Material

Refer to Web version on PubMed Central for supplementary material.

Acknowledgments

Research reported in this publication was supported by the Yale SPORE in Skin Cancer, funded by the National Cancer Institute, US National Institutes of Health, under award number 1 P50 CA121974 (R.H.); the Melanoma Research Alliance (Team award to R.H., M.B. and M.K.); Gilead Sciences, Inc. (J.S. and R.H.); the Howard Hughes Medical Institute (R.P.L.); the Department of Dermatology; and the Yale Comprehensive Cancer Center. The content of this article is solely the responsibility of the authors and does not necessarily represent the official views of the US National Institutes of Health.

References

1. Davis MJ, et al. RAC1P29S is a spontaneously activating cancer-associated GTPase. Proc. Natl. Acad. Sci. USA. 2013; 110: 912–917. [PubMed: 23284172]
2. Hodis E, et al. A landscape of driver mutations in melanoma. Cell. 2012; 150: 251–263. [PubMed: 22817889]
3. Krauthammer M, et al. Exome sequencing identifies recurrent somatic *RAC1* mutations in melanoma. Nat. Genet. 2012; 44: 1006–1014. [PubMed: 22842228]
4. Gold HL, et al. PP6C hotspot mutations in melanoma display sensitivity to Aurora kinase inhibition. Mol. Cancer Res. 2014; 12: 433–439. [PubMed: 24336958]
5. Hammond D, et al. Melanoma-associated mutations in protein phosphatase 6 cause chromosome instability and DNA damage owing to dysregulated Aurora-A. J. Cell Sci. 2013; 126: 3429–3440. [PubMed: 23729733]
6. Prickett TD, et al. Exon capture analysis of G protein–coupled receptors identifies activating mutations in *GRM3* in melanoma. Nat. Genet. 2011; 43: 1119–1126. [PubMed: 21946352]
7. Stark MS, et al. Frequent somatic mutations in *MAP3K5* and *MAP3K9* in metastatic melanoma identified by exome sequencing. Nat. Genet. 2012; 44: 165–169.
8. Huang FW, et al. Highly recurrent TERT promoter mutations in human melanoma. Science. 2013; 339: 957–959. [PubMed: 23348506]
9. Horn S, et al. TERT promoter mutations in familial and sporadic melanoma. Science. 2013; 339: 959–961. [PubMed: 23348503]
10. Martin M, et al. Exome sequencing identifies recurrent somatic mutations in *EIF1AX* and *SF3B1* in uveal melanoma with disomy 3. Nat. Genet. 2013; 45: 933–936. [PubMed: 23793026]
11. Harbour JW, et al. Frequent mutation of BAP1 in metastasizing uveal melanomas. Science. 2010; 330: 1410–1413. [PubMed: 21051595]
12. Vogelstein B, et al. Cancer genome landscapes. Science. 2013; 339: 1546–1558. [PubMed: 23539594]
13. Lawrence MS, et al. Mutational heterogeneity in cancer and the search for new cancer-associated genes. Nature. 2013; 499: 214–218. [PubMed: 23770567]
14. Cancer Genome Atlas Network. Genomic classification of cutaneous melanoma. Cell. 2015; 161: 1681–1696. [PubMed: 26091043]

15. Guen VJ, et al. CDK10/cyclin M is a protein kinase that controls ETS2 degradation and is deficient in STAR syndrome. Proc. Natl. Acad. Sci. USA. 2013; 110: 19525–19530. [PubMed: 24218572]
16. Chou CH, et al. GSK3β regulates Bcl2L12 and Bcl2L12A anti-apoptosis signaling in glioblastoma and is inhibited by LiCl. Cell Cycle. 2012; 11: 532–542. [PubMed: 22262180]
17. Gartner JJ, et al. Whole-genome sequencing identifies a recurrent functional synonymous mutation in melanoma. Proc. Natl. Acad. Sci. USA. 2013; 110: 13481–13486. [PubMed: 23901115]
18. Zang ZJ, et al. Exome sequencing of gastric adenocarcinoma identifies recurrent somatic mutations in cell adhesion and chromatin remodeling genes. Nat. Genet. 2012; 44: 570–574. [PubMed: 22484628]
19. McHugh JB, Fullen DR, Ma L, Kleer CG, Su LD. Expression of polycomb group protein EZH2 in nevi and melanoma. J. Cutan. Pathol. 2007; 34: 597–600. [PubMed: 17640228]
20. Dillon SC, Zhang X, Trievel RC, Cheng X. The SET-domain protein superfamily: protein lysine methyltransferases. Genome Biol. 2005; 6: 227. [PubMed: 16086857]
21. Duns G, et al. Histone methyltransferase gene *SETD2* is a novel tumor suppressor gene in clear cell renal cell carcinoma. Cancer Res. 2010; 70: 4287–4291. [PubMed: 20501857]
22. Wei X, et al. Exome sequencing identifies GRIN2A as frequently mutated in melanoma. Nat. Genet. 2011; 43: 442–446. [PubMed: 21499247]
23. Wu Q, et al. 27-Hydroxycholesterol promotes cell-autonomous, ER-positive breast cancer growth. Cell Rep. 2013; 5: 637–645. [PubMed: 24210818]
24. Yan H, et al. *IDH1* and *IDH2* mutations in gliomas. N. Engl. J. Med. 2009; 360: 765–773. [PubMed: 19228619]
25. Jin G, et al. Disruption of wild-type IDH1 suppresses D-2-hydroxyglutarate production in *IDH1*-mutated gliomas. Cancer Res. 2013; 73: 496–501. [PubMed: 23204232]
26. Yarwood S, Bouyoucef-Cherchalli D, Cullen PJ, Kupzig S. The GAP1 family of GTPase-activating proteins: spatial and temporal regulators of small GTPase signalling. Biochem. Soc. Trans. 2006; 34: 846–850. [PubMed: 17052212]
27. Chen PC, et al. Next-generation sequencing identifies rare variants associated with Noonan syndrome. Proc. Natl. Acad. Sci. USA. 2014; 111: 11473–11478. [PubMed: 25049390]
28. Ratner N, Miller SJA. RASopathy gene commonly mutated in cancer: the neurofibromatosis type 1 tumour suppressor. Nat. Rev. Cancer. 2015; 15: 290–301. [PubMed: 25877329]
29. Kontaridis MI, Swanson KD, David FS, Barford D, Neel BG. PTPN11 (Shp2) mutations in LEOPARD syndrome have dominant negative, not activating, effects. J. Biol. Chem. 2006; 281: 6785–6792. [PubMed: 16377799]
30. Tartaglia M, et al. Diversity and functional consequences of germline and somatic *PTPN11* mutations in human disease. Am. J. Hum. Genet. 2006; 78: 279–290. [PubMed: 16358218]
31. Lepri F, et al. *SOS1* mutations in Noonan syndrome: molecular spectrum, structural insights on pathogenic effects, and genotype-phenotype correlations. Hum. Mutat. 2011; 32: 760–772. [PubMed: 21387466]
32. Tartaglia M, et al. Gain-of-function *SOS1* mutations cause a distinctive form of Noonan syndrome. Nat. Genet. 2007; 39: 75–79. [PubMed: 17143282]
33. Roberts AE, et al. Germline gain-of-function mutations in *SOS1* cause Noonan syndrome. Nat. Genet. 2007; 39: 70–74. [PubMed: 17143285]
34. Pandit B, et al. Gain-of-function *RAF1* mutations cause Noonan and LEOPARD syndromes with hypertrophic cardiomyopathy. Nat. Genet. 2007; 39: 1007–1012. [PubMed: 17603483]
35. Stowe IB, et al. A shared molecular mechanism underlies the human rasopathies Legius syndrome and Neurofibromatosis-1. Genes Dev. 2012; 26: 1421–1426. [PubMed: 22751498]
36. Brems H, et al. Review and update of SPRED1 mutations causing Legius syndrome. Hum. Mutat. 2012; 33: 1538–1546. [PubMed: 22753041]
37. Ostman A, Hellberg C, Bohmer FD. Protein-tyrosine phosphatases and cancer. Nat. Rev. Cancer. 2006; 6: 307–320. [PubMed: 16557282]
38. Ko JM, Kim JM, Kim GH, Yoo HW. *PTPN11, SOS1, KRAS*, and *RAF1* gene analysis, and genotype-phenotype correlation in Korean patients with Noonan syndrome. J. Hum. Genet. 2008; 53: 999–1006. [PubMed: 19020799]

39. Tanoue T, Adachi M, Moriguchi T, Nishida E. A conserved docking motif in MAP kinases common to substrates, activators and regulators. Nat. Cell Biol. 2000; 2: 110–116. [PubMed: 10655591]
40. Janakiraman M, et al. Genomic and biological characterization of exon 4 *KRAS* mutations in human cancer. Cancer Res. 2010; 70: 5901–5911. [PubMed: 20570890]
41. Johnson DB, et al. Combined BRAF (dabrafenib) and MEK inhibition (trametinib) in patients with BRAFV600-mutant melanoma experiencing progression with single-agent BRAF inhibitor. J. Clin. Oncol. 2014; 32: 3697–3704. [PubMed: 25287827]
42. Chapman PB, et al. Improved survival with vemurafenib in melanoma with BRAF V600E mutation. N. Engl. J. Med. 2011; 364: 2507–2516. [PubMed: 21639808]
43. Whittaker SR, et al. A genome-scale RNA interference screen implicates NF1 loss in resistance to RAF inhibition. Cancer Discov. 2013; 3: 350–362. [PubMed: 23288408]
44. Nissan MH, et al. Loss of NF1 in cutaneous melanoma is associated with RAS activation and MEK dependence. Cancer Res. 2014; 74: 2340–2350. [PubMed: 24576830]
45. Ranzani M, et al. BRAF/NRAS wild-type melanoma, NF1 status and sensitivity to trametinib. Pigment Cell Melanoma Res. 2015; 28: 117–119. [PubMed: 25243813]
46. Magi A, et al. EXCAVATOR: detecting copy number variants from whole-exome sequencing data. Genome Biol. 2013; 14: R120. [PubMed: 24172663]
47. Beroukhim R, et al. Assessing the significance of chromosomal aberrations in cancer: methodology and application to glioma. Proc. Natl. Acad. Sci. USA. 2007; 104: 20007–20012. [PubMed: 18077431]
48. Ji Z, Flaherty KT, Tsao H. Targeting the RAS pathway in melanoma. Trends Mol. Med. 2012; 18: 27–35. [PubMed: 21962474]
49. Shibuya M. VEGFR and type-V RTK activation and signaling. Cold Spring Harb. Perspect. Biol. 2013; 5: a009092. [PubMed: 24086040]
50. Johannessen CM, et al. COT drives resistance to RAF inhibition through MAP kinase pathway reactivation. Nature. 2010; 468: 968–972. [PubMed: 21107320]
51. Watson IR, et al. The RAC1 P29S hotspot mutation in melanoma confers resistance to pharmacological inhibition of RAF. Cancer Res. 2014; 74: 4845–4852. [PubMed: 25056119]
52. Newton AC, Trotman LC. Turning off AKT: PHLPP as a drug target. Annu. Rev. Pharmacol. Toxicol. 2014; 54: 537–558. [PubMed: 24392697]
53. Dong L, et al. Oncogenic suppression of PHLPP1 in human melanoma. Oncogene. 2014; 33: 4756–4766. [PubMed: 24121273]
54. Gallino G, et al. Association between cutaneous melanoma and neurofibromatosis type 1: analysis of three clinical cases and review of the literature. Tumori. 2000; 86: 70–74. [PubMed: 10778770]
55. Seminog OO, Goldacre MJ. Risk of benign tumours of nervous system, and of malignant neoplasms, in people with neurofibromatosis: population-based record-linkage study. Br. J. Cancer. 2013; 108: 193–198. [PubMed: 23257896]
56. De Schepper S, et al. Somatic mutation analysis in NF1 cafe au lait spots reveals two NF1 hits in the melanocytes. J. Invest. Dermatol. 2008; 128: 1050–1053. [PubMed: 17914445]
57. Johnson MR, Look AT, DeClue JE, Valentine MB, Lowy DR. Inactivation of the *NF1* gene in human melanoma and neuroblastoma cell lines without impaired regulation of GTP.Ras. Proc. Natl. Acad. Sci. USA. 1993; 90: 5539–5543. [PubMed: 8516298]
58. Andersen LB, et al. Mutations in the neurofibromatosis 1 gene in sporadic malignant melanoma cell lines. Nat. Genet. 1993; 3: 118–121. [PubMed: 8499944]
59. Marees T, et al. Cancer mortality in long-term survivors of retinoblastoma. Eur. J. Cancer. 2009; 45: 3245–3253. [PubMed: 19493675]
60. Nyström AM, et al. A severe form of Noonan syndrome and autosomal dominant cafe-au-lait spots —evidence for different genetic origins. Acta Paediatr. 2009; 98: 693–698. [PubMed: 19120036]
61. Prada CE, et al. Lethal presentation of neurofibromatosis and Noonan syndrome. Am. J. Med. Genet. A. 2011; 155A: 1360–1366. [PubMed: 21567923]
62. Thiel C, et al. Independent *NF1* and *PTPN11* mutations in a family with neurofibromatosis-Noonan syndrome. Am. J. Med. Genet. A. 2009; 149A: 1263–1267. [PubMed: 19449407]

63. Stites EC, Trampont PC, Haney LB, Walk SF, Ravichandran KS. Cooperation between noncanonical Ras network mutations. Cell Rep. 2015; 10: 307–316. [PubMed: 25600866]

References

64. Halaban R, et al. PLX4032, a selective BRAF(V600E) kinase inhibitor, activates the ERK pathway and enhances cell migration and proliferation of BRAF melanoma cells. Pigment Cell Melanoma Res. 2010; 23: 190–200. [PubMed: 20149136]

65. Li H, Durbin R. Fast and accurate short read alignment with Burrows-Wheeler transform. Bioinformatics. 2009; 25: 1754–1760. [PubMed: 19451168]

66. Li H, et al. The Sequence Alignment/Map format and SAMtools. Bioinformatics. 2009; 25: 2078–2079. [PubMed: 19505943]

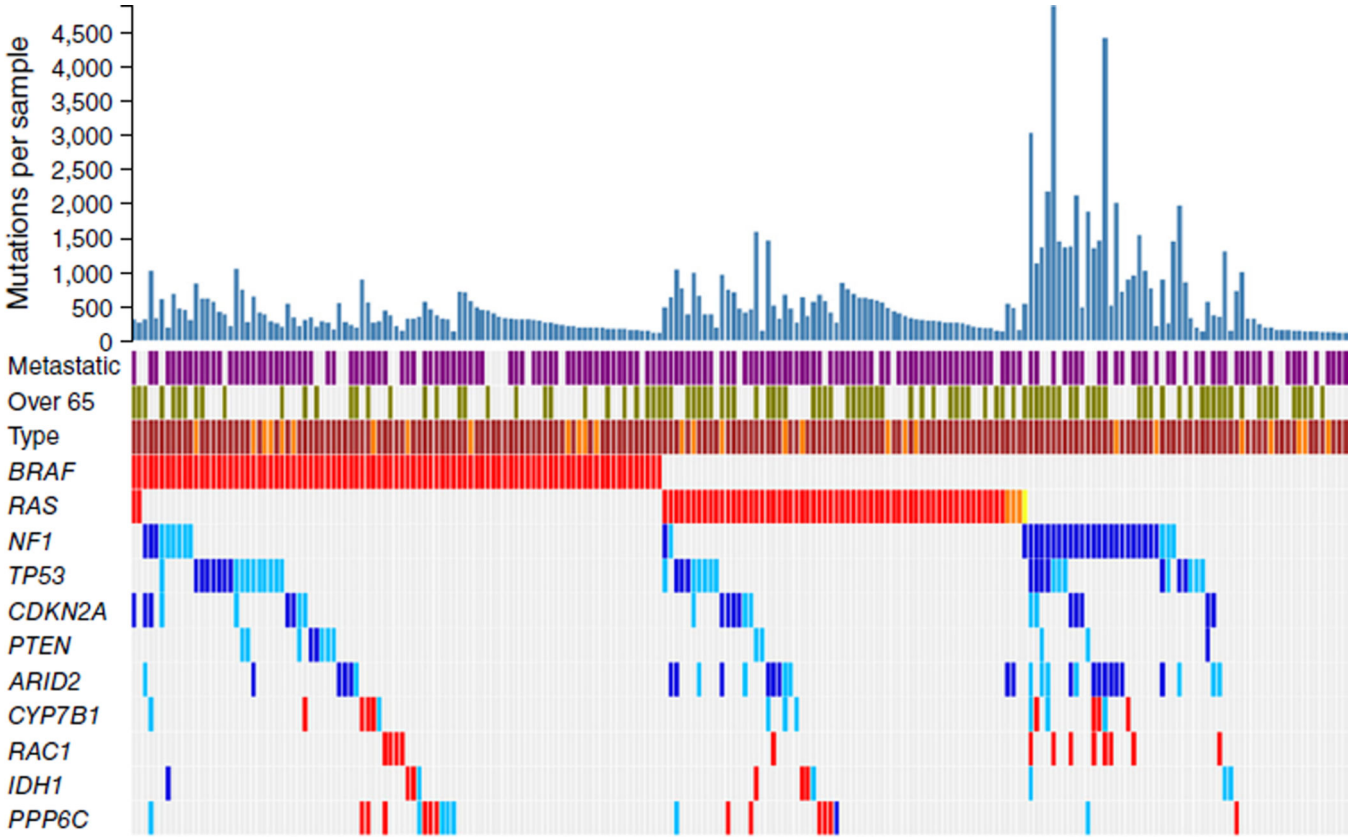

Figure 1.

Melanoma mutational landscape (n = 213). Top 11 melanoma-driver genes that reach genome-wide significance according to background mutation-frequency estimation. Purple, metastatic melanoma; green, patients over 65 years old; red, mutations at recurrent positions; dark blue, inactivating mutations (nonsense, splice, indel); light blue, predicted harmful mutations. Brown and darker orange represent sun-exposed tumors and tumors of unknown origin, respectively. Mutations in *HRAS* and *KRAS* are marked in light orange and yellow, respectively. Mutation counts correspond to novel mutations that are not found in repositories of common human variants.

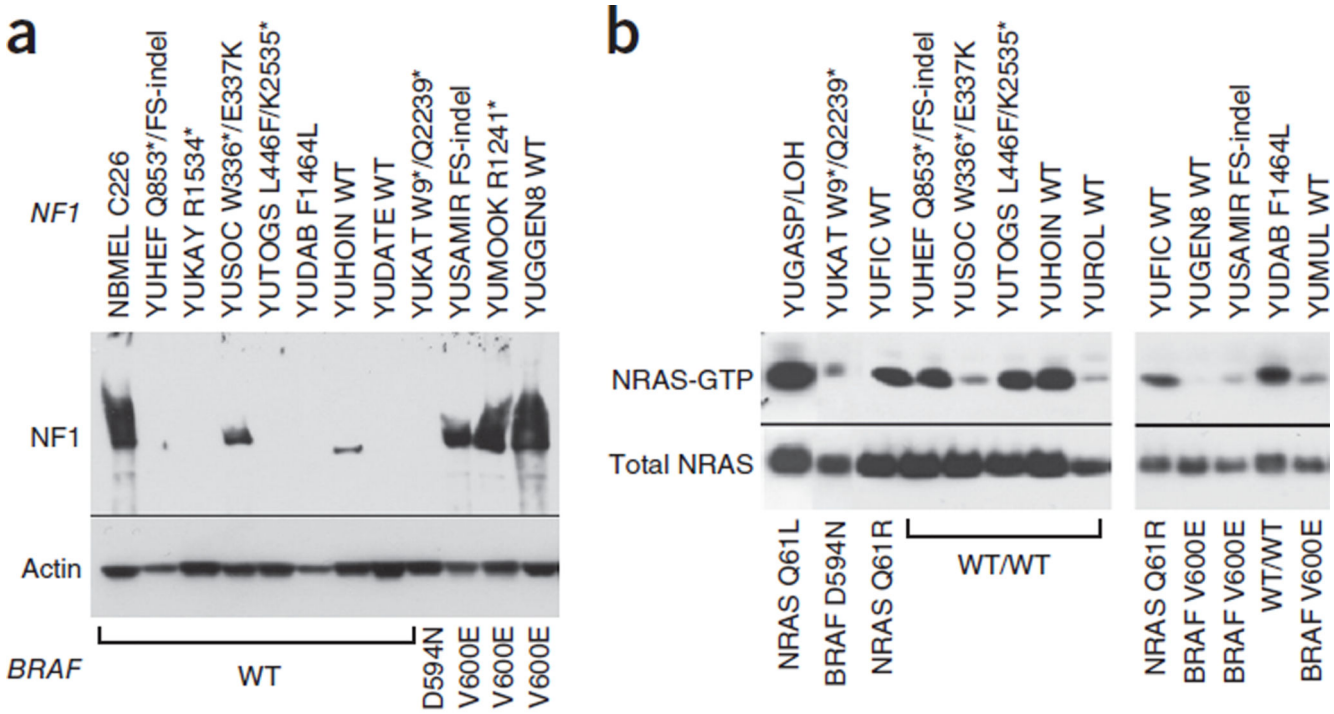

c

Sample	*BRAF-RAS*	*NF1*	NF1 expression	RAS relative activity
YUGASP	*NRAS*^{Q61L}	WT	Low	1.74
YUDAB	WT	F1464L	Null	1.22
YUFIC	*NRAS*^{Q61R}	WT	Expressed	1.00
YUHOIN	WT	WT	Low	0.92
YUTOGS	WT	L446F/K2535*	Null	0.77
YUHEF	WT	Q853*/FS-indel	Null	0.69
YUMUL	*BRAF*^{V600E}	WT	Expressed	0.34
YUKAT	WT	W9*/Q2239*	Null	0.29
YUSAMIR	*BRAF*^{V600E}	FS-indel	Expressed	0.14
YUSOC	WT	W336*/E337K	Low	0.12
YUROL	WT	WT	Expressed	0.10
YUGEN8	*BRAF*^{V600E}	WT	Expressed	0.03

Figure 2.

NF1 expression and NRAS activity. (**a**) Protein blot showing NF1 expression in melanoma cells (YU designation) relative to that in normal human melanocytes (NBMEL) derived from a single newborn foreskin; β-actin was used as a loading control. *NF1* mutations are indicated at the top, and *BRAF* mutations at the bottom. The wild-type NF1 (WT) melanomas YUHOIN and YUDATE displayed LOH. All the melanoma cell lines represented in this panel are NRAS wild type. The reproducibility data and protein expression in additional representative melanoma cell lines are presented in Supplementary

Figure 4. (**b**) NRAS activity as determined by NRAS-GTP pulldown assay showing active NRAS-GTP and total NRAS detected in lysates. The same results were obtained with pan-RAS antibodies (data not shown). (**c**) Ranking of NRAS activity with *BRAF, NRAS* and *NF1* mutation and expression status. We derived numbers by scanning the bands and quantitating the bands' intensity relative to input NRAS using ImageJ and normalizing against the $NRAS^{Q61R}$ YUFIC melanoma. FS, frame shift.

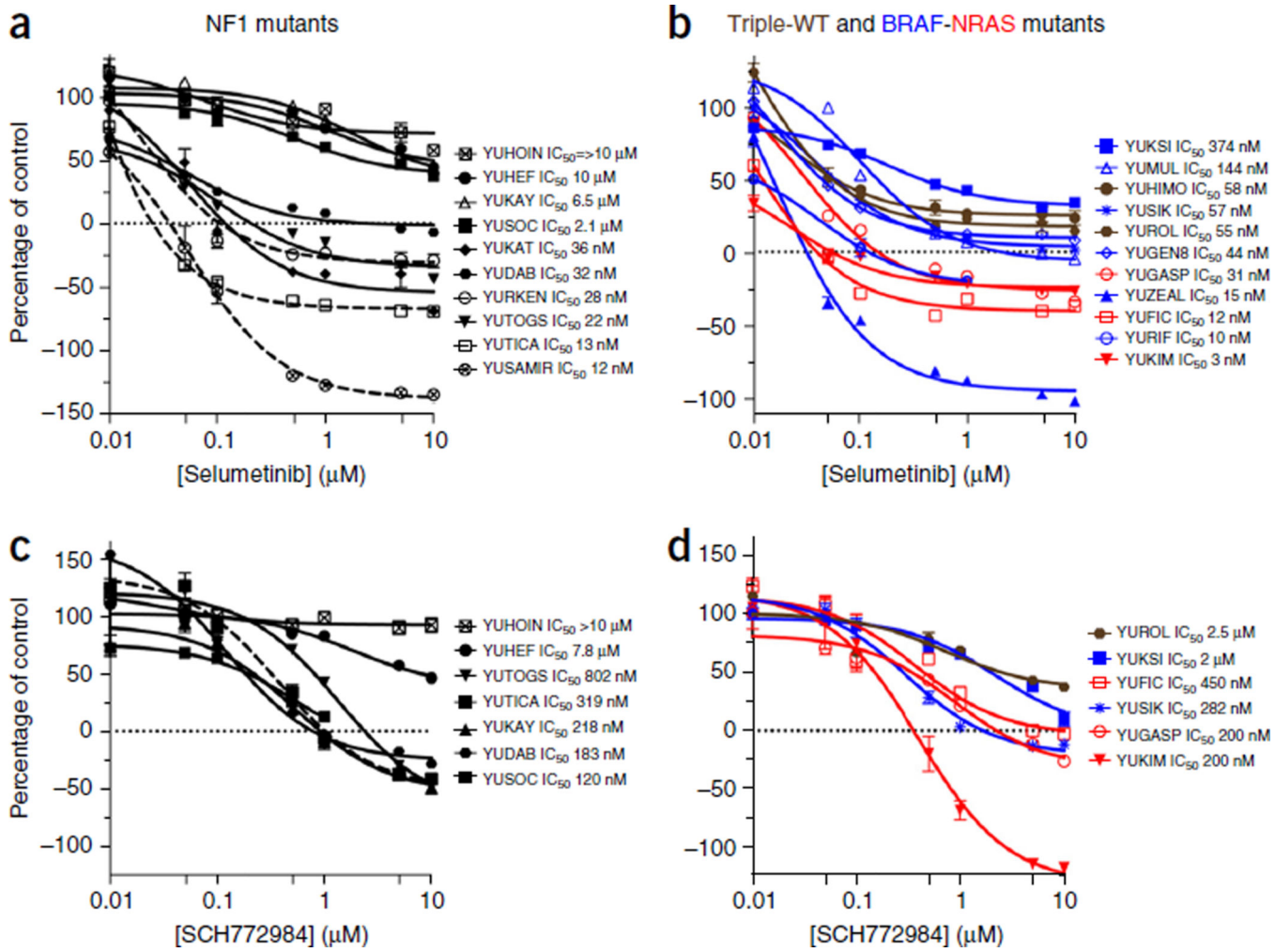

Figure 3.

Growth responses to selumetinib and SCH772984. (**a–d**) Growth of NF1-mutant (**a,c**) and of triple–wild-type (brown), *BRAF*^{V600}-mutant (blue) and *NRAF*^{SQ61}-mutant (red) melanoma cell lines (**b,d**). In **a**, the NF1 mutants YURKEN, YUTICA and YUSAMIR (dashed lines) are double-mutant cell lines (*BRAF*^{V600E}, *NRAS*^{Q61R} and *BRAF*^{V600E}, respectively) that express normal levels of NF1. The rest of the lines are null for NF1 (Fig. 2a). The selumetinib experiments were repeated at least twice. The data represent cell viability (CellTiter-Glo luminescent assay) as a percentage of the control at the end of 72 h of treatment. Each measurement is the average of triplicate or quadruplet wells. Error bars denote s.e.m.

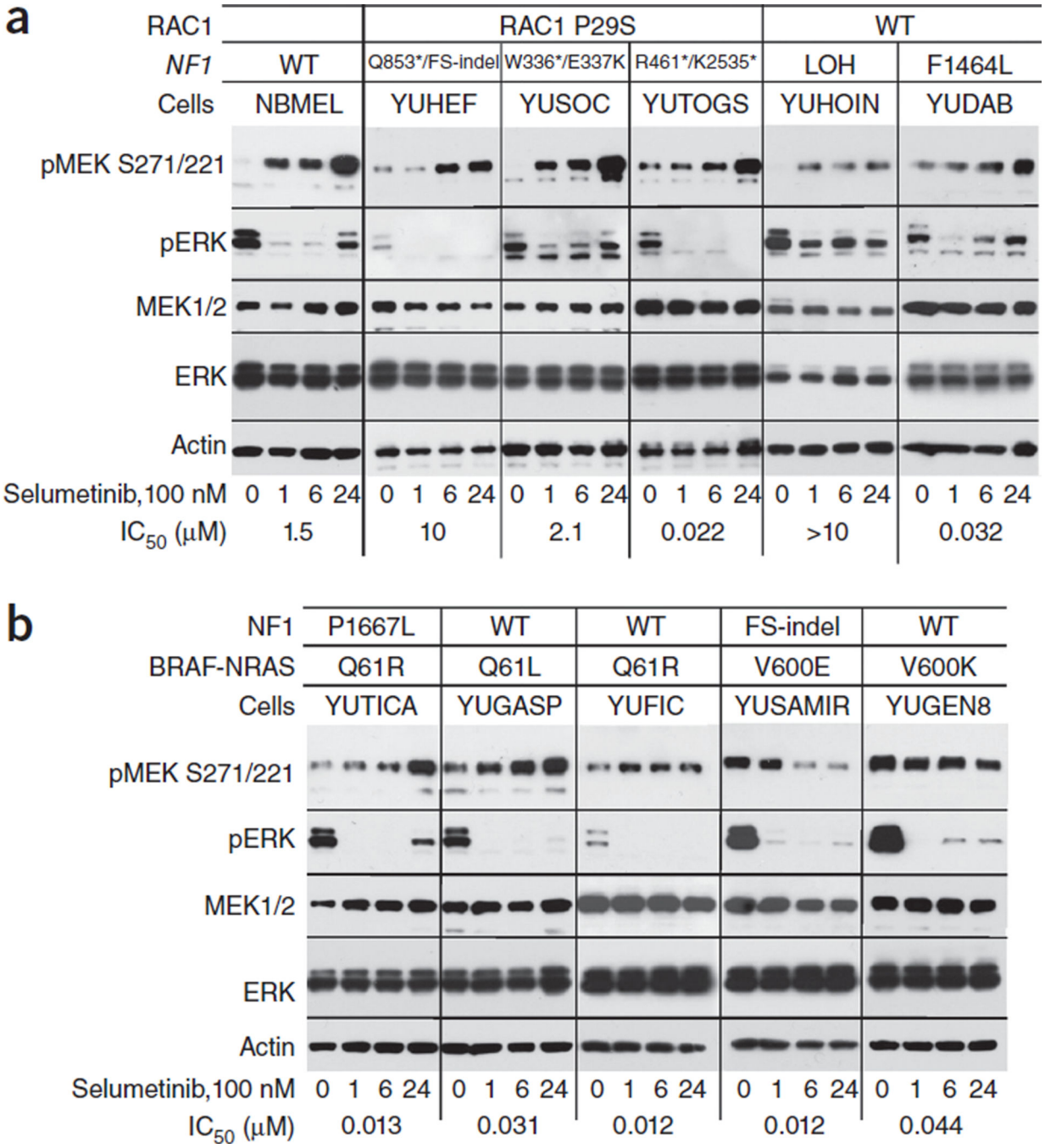

Figure 4.

Changes in MEK1/2 and ERK phosphorylation in response to selumetinib. Normal human melanocytes (NBMEL) and melanoma cell lines were untreated (0) or treated with 100 nM selumetinib for 1, 6 and 24 h. The panels show protein blots probed with the indicated antibodies. (**a**) Normal melanocytes and NF1-mutant melanoma cell lines that are wild type for BRAF and NRAS. (**b**) Melanoma cell lines that are NF1, NRAS or BRAF mutants, as indicated. Numbers on the bottom show the IC_{50} in response to selumetinib (Fig. 3). The types of *NF1* and *RAC1* mutations are indicated for each cell line at the top.

All the cell lines in **b** express wild-type RAC1. Figure 2a and supplementary Figure 4 show the corresponding levels of NF1 expression. The results represent one of two similar experiments.

Table 1

Top mutated genes across the Yale cohort ($n = 213$)

Symbol	Samples with mutations at recurrent positions	Incidence (%)	Symbol	Samples with inactivating mutations	Incidence (%)
BRAF	93	43.7	*NF1*	28	13.1
NRAS	62	29.1	*ARID2*	20	9.4
RAC1	13	6.1	*TP53*	17	8.0
PPP6C	12	5.6	*CDKN2A*	11	5.2
GABRA3	11	5.2	*KMT2B*	9	4.2
ABCB5	9	4.2	*ATM*	6	2.8
TRRAP	8	3.8	*ASPM*	5	2.3
CYP7B1	8	3.8	*ARID1A*	5	2.3
PCDHGA1	7	3.3	*RB1*	4	1.9
DGKI	7	3.3	*TNRC6B*	4	1.9
KNSTRN	6	2.8	*SETD2*	4	1.9
BCL2L12	5	2.3	*FAM58A*	4	1.9
IDH1	5	2.3	*ITGA5*	4	1.9
PLCE1	5	2.3	*NIN*	4	1.9
LTN1	5	2.3	*SPRED1*	4	1.9
MAP2K1	4	1.9	*OAS3*	4	1.9
RQCD1	4	1.9	*USP24*	4	1.9
PROS1	4	1.9	*PTEN*	3	1.4
EZH2	4	1.9	*MME*	3	1.4
FRMD4B	4	1.9	*YLPM1*	3	1.4

The list shows the top 40 expressed genes with high mutation burdens according to the 20/20 rule[12]. The rule identifies genes with mutations at recurrent positions that constitute 20% or more of all observed mutations as likely oncogenes (three leftmost columns) and genes with at least 20% inactivating mutations (i.e., premature termination, splice-site variant or indel) as likely tumor suppressors (three rightmost columns). Also shown is the number of samples with qualifying mutations in these genes.

Table 2

Mutational status of the Yale cohort (n = 213)

			RAS				
		BRAF	***NRAS***	***HRAS***	***KRAS***	***NF1***	**WT**
BRAF		82 (38.5%)					
RAS	*NRAS*	2 (0.9%)	58 (27.2%)				
	HRAS	0	0	3 (1.4%)			
	KRAS	0	0	0	0		
NF1		9 (4.2%)	2 (0.9%)	0	1 (0.5%)	26 (12.2%)	
WT		0	0	0	0	0	30 (14.1%)

Breakdown by activating mutations in *BRAF* (p.Val600) and *RAS* (p.Gln61/Gly12/Gly13) and inactivating mutations (stop mutations, splice-site variants, indels) and predicted damaging *NF1* mutations. WT, triple–wild-type melanomas.

Table 3

Co-mutations in RASopathy genes in *NF1*-mutant, *BRAF-RAS*–wild-type melanomas in the Yale cohort

Sample	*NF1* mutations	RASopathy gene mutations
YUBER	p.Arg262Cys, p.Trp784*	*SOS1* ^{G434R}
YUCAS	p.Ile679AspfsX21	–
YUDAB	p.Phe1464Leu	*PTPN11* ^{Q506P}
YUFIGUR	p.Tyr628LeufsX6, p.Gln2234*	–
YUHEF	p.Lys2552ThrfsX2, p.Gln853*	*SOS1* ^{G434V,R398H,P102S}, *RAF1* ^{P261L}
YUKAT	p.Trp9*, p.Gln2239*	*SOS1* ^{R1067G}
YUKAY	p.Arg1534*	–
YUKLAB	p.Ser2025Leu, p.Arg1204Trp, p.Arg416*	*PTPN11* ^{P491L,Q510L,D425N}, *RASA2* ^{P530L}
YULAN	NF1: c.6819+1G>A, p.Pro1084Ser	–
YUMUJ	p.Lys1632MetfsX8	*PTPN11* ^{A461T}
YUNEKI	p.Gln803*	–
YUOMEGA	p.Asn793LysfsX14, p.Leu844Phe	*SPRED1* ^{R117Q}
YUOTHO	p.Gln1010*, pGln2239*	*RASA2* ^{S400F}
YUPADI	p.Ser2093Phe, p.Arg1362*	*SPRED1* ^{Q353*}
YUPAER	p.Gln912*	–
YUPAT	p.Leu844Phe	–
YUPROST	p.Arg440*	*RASA2* ^{R310*}
YURAY	p.Arg2450*	–
YUROG	p.Gln1218*	–
YUROO	p.Gln282*, p.Arg440* p.Leu2661*	*RASA2* ^{F585I}
YURUS	p.Gln2434*	*RASA2* ^{R511C,P843S}, *SPRED1* ^{Q205*}
YUSOC	p.Glu337Lys, pTrp336*	*RASA2* ^{R511C,Q500*}, *RAF1* ^{T491I}
YUTAR	p.Val2653SerfsX26	*RASA2* ^{R511C}
YUTOGS	p.Leu466Phe, p.Lys2535*	–
YUWAND	p.Phe694_Trp696del	*PTN11* ^{Y279C}, *SOS1* ^{R552K}
YUZAN	p.Met108Ile	–

Mutations in *RASA2* (pArg511Cys), *PTPN11* (p.Tyr279Cys, p.Ala461Thr, p.Pro491Leu, p.Gln506Pro), *SOS1* (p.Gly434Arg, p.Arg552Lys) and *RAF1* (p.Pro261Leu, p.Thr491Ile) have been previously shown to be disease causing in RASopathy syndromes (see text for details).